Efficient chito-oligosaccharide utilization requires two TonB-dependent transporters and one hexosaminidase in *Cellvibrio japonicus*

Estela C. Monge and Jeffrey G. Gardner[#]

Running Title
Chito-oligosaccharide utilization by *C. japonicus*

Keywords:
Cellvibrio japonicus, chitin, glycoside hydrolase, hexosaminidase, TonB-dependent transporter

Author Affiliations
Department of Biological Sciences, University of Maryland - Baltimore County, Baltimore, Maryland, USA

[#] **Correspondence**
Jeffrey G. Gardner
Department of Biological Sciences
University of Maryland - Baltimore County
Email: jgardner@umbc.edu
Phone: 410-455-3613
Fax: 410-455-3875

SUMMARY

Chitin utilization by microbes plays a significant role in biosphere carbon and nitrogen cycling, and studying the microbial approaches used to degrade chitin will facilitate our understanding of bacterial strategies to degrade a broad range of recalcitrant polysaccharides. The early stages of chitin depolymerization by the bacterium *Cellvibrio japonicus* have been characterized and are dependent on one chitin-specific lytic polysaccharide monooxygenase and non-redundant glycoside hydrolases from the family GH18 to generate chito-oligosaccharides for entry into metabolism. Here, we describe the mechanisms for the latter stages of chitin utilization by *C. japonicus* with an emphasis on the fate of chito-oligosaccharides. Our systems biology approach combined transcriptomics and bacterial genetics using ecologically relevant substrates to determine the essential mechanisms for chito-oligosaccharide transport and catabolism in *Cellvibrio japonicus*. Using RNAseq analysis we found a coordinated expression of genes that encode polysaccharide-degrading enzymes. Mutational analysis determined that the *hex20B* gene product, predicted to encode a hexosaminidase, was required for efficient utilization of chito-oligosaccharides. Furthermore, two gene loci (CJA_0353 and CJA_1157), which encode putative TonB-dependent transporters, were also essential for chito-oligosaccharides utilization. This study further develops our model of *C. japonicus* chitin metabolism and may be predictive for other environmentally or industrially important bacteria.

INTRODUCTION

Chitin is an environmentally abundant β-(1-4)-linked *N*-acetylglucosamine (GlcNAc) homopolymer that is a major contributor to global carbon and nitrogen cycles. Found in both marine and terrestrial ecosystems, the efficient depolymerization of chitin is driven by microbes resulting in little environmental accumulation of chitin degradation products (Beier & Bertilsson, 2013, Gooday, 1990). In addition to its ecological importance, chitin and its degradation products are of increasing interest to the biotechnology industry due to their potential as a feedstock for renewable fuels and chemicals (Zhu *et al.*, 2004, Satari & Karimi, 2018, Gopal *et al.*, 2019, Khor & Lim, 2003, Francesko & Tzanov, 2011, Matroodi *et al.*, 2013). While there are three isomorphs of chitin, the dominant form found in nature is α-chitin, which is found in fungi, insects, and crustaceans (Ifuku, 2014, Moussian, 2019).

Despite the promise of chitin-containing biomass, the industrial degradation of this polymer has been described as inefficient and wasteful using current methods (Yan & Chen, 2015). Consequently, there has been renewed interest in elucidating the approaches bacteria and fungi employ to degrade chitin-containing substrates because this process is highly efficient (Tharanathan & Kittur, 2003, Gortari & Hours, 2013). This efficiency is the result of potent Carbohydrate Active EnZymes (CAZymes; [http://www.cazy.org]) (Lombard *et al.*, 2014), specifically lytic polysaccharide monooxygenases (LPMOs) and glycoside hydrolases (GHs). The LPMOs from family AA10 are known to act on chitin and disrupt its crystalline structure (Vaaje-Kolstad *et al.*, 2005). Glycoside hydrolase families with known chitin-degrading activities (GH18, GH19, and GH46) then cleave soluble chitin polymers into chito-oligosaccharides.

These oligosaccharides are then subsequently cleaved to free GlcNAc monomers by enzymes from the GH3, GH20, and GH84 families (Stoykov *et al.*, 2015, Nguyen *et al.*, 2018).

One of the reasons postulated for the large number of CAZymes required to degrade chitin-containing biomass is the complex and insoluble nature of these substrates. For example, the shells of crabs are considered a type of recalcitrant biomass due to its complex composition. Specifically, the exoskeleton of these crustaceans is hierarchically organized and includes chitin nanofibers bundled by proteins, which are subsequently encased in calcium carbonate (Raabe *et al.*, 2005). The degradation of complex substrates such as crustacean shells has been previously studied, and there are currently several bacterial models of chitin degradation (Vaaje-Kolstad *et al.*, 2013, Meibom *et al.*, 2004, Lacombe-Harvey *et al.*, 2018).

One bacterial model system that has recently emerged with robust systems biology methods to study recalcitrant polysaccharide degradation is *Cellvibrio japonicus* (Gardner, 2016, Attia et al., 2018, Garcia et al., 2020). This bacterium has been previously shown as proficient at chitin degradation (Forsberg *et al.*, 2016, Tuveng *et al.*, 2016, Monge *et al.*, 2018) and has nine predicted chitin specific genes, which include four family GH18 enzymes, one GH19 enzyme, two GH20 enzymes, one GH46 enzyme, and one chitin-specific AA10 LPMO (DeBoy *et al.*, 2008). Previous transcriptomic, genetic (Monge *et al.*, 2018), and proteomic studies (Tuveng *et al.*, 2016) confirmed the importance of the GH18 enzymes and the LPMO for chitin degradation (Forsberg *et al.*, 2016). Interestingly, despite having four GH18 enzymes only the Chi18D chitinase was essential for chitin degradation in *C. japonicus*.

Additionally, the LPMO was critical in the early stages of degradation and acted on the highly insoluble and crystalline portions of chitin.

Building upon that previous work, here we report the mechanism of chito-oligosaccharide uptake and catabolism by *C. japonicus*. We determined that the genes *cttA* (CJA_0353) and *cttB* (CJA_01157) encode TonB-dependent transporters, which are essential for the transport of chito-oligosaccharides into the periplasm. Using a combination of mutational analysis and heterologous expression we determined that the gene product of *hex20B* is a hexosaminidase that generates GlcNAc from chito-oligosaccharides. These findings refine our model of *C. japonicus* chitin utilization, which suggests sophisticated regulation to secrete a battery of CAZymes that perform the initial stages of chitin degradation extracellularly. Using highly efficient transport systems the bacterium then imports chito-oligosaccharides into the periplasmic space for conversion to GlcNAc and entry into metabolism. This method of chitin utilization ensures a strong return on investment for the energy spent to produce and then secrete a large number of CAZymes.

RESULTS

Transcriptome analysis of *C. japonicus* reveals a complex regulatory response during the degradation of chitin-containing substrates. A previous RNAseq study using purified α-chitin as a substrate observed the up-regulation of all nine genes that encode enzymes with predicted chitinolytic activities from *C. japonicus*, but interestingly also a variety of CAZyme genes implicated in the degradation of other polysaccharides (Monge *et al.*, 2018). Therefore, we hypothesized that *C. japonicus* has a complex regulatory network to control the expression of CAZymes. Additionally, we wanted to determine if the gene expression response for *C. japonicus* CAZymes would be altered when utilizing an environmentally relevant complex substrate. Therefore, we analyzed the gene expression patterns of *C. japonicus* grown using crab shells as a model complex substrate in addition to testing glucose (Glc), *N*-acetylglucosamine (GlcNAc), and purified α-chitin. Specifically, we wanted to determine the differences in gene expression that were dependent on substrate and growth phase of *C. japonicus*, and consequently our cut-off parameters for the RNAseq analysis was consistent across comparisons (2-fold change in gene expression with a p-value of 0.01 were deemed significant).

For our initial analysis, we compared the gene expression profile of cells grown using GlcNAc versus cells grown using Glc during exponential growth. From this analysis, we identified only 42 genes that were up-regulated for cells grown using GlcNAc, including six that were CAZyme-encoding genes with predicted activity on chitin or GlcNAc (*nag9A*, *hex20B*, *chi18D*, *chi18C*, *chi18A*, and *chi18B*). Interestingly, a gene with the locus tag CJA_1157 was the most up-regulated transcript in the GlcNAc

condition and is predicted to encode an outer membrane transporter. A second outer membrane transporter with the locus tag CJA_0353 was also up-regulated. Additionally, a putative operon that encodes two inner membrane transporters (*gluP*, locus ID: CJA_1161) and CJA_1162**)**, a sugar deacetylase (*nag9A,* locus ID: CJA_1163), and a sugar deaminase (*nagB,* locus ID: CJA_1164) were up-regulated in the GlcNAc condition (**Fig. 1A, Fig. 2,** & **Table S1A**).

When we compared the transcriptomic profile of GlcNAc versus Glc cells in stationary phase, we observed a total of 500 genes that were up-regulated in GlcNAc, but only four were CAZyme genes. Of the chitin relevant genes, only *chi18A* was up-regulated. The transporter CJA_1157 was up-regulated while there was no change in the expression of CJA_0353. Two of the genes of the GlcNAc operon were also up-regulated (*gluP* and *nag9A*) **(Fig. S1A** & **Table S2A)**. We also compared gene expression between exponential growth versus stationary phase for cells grown using GlcNAc and observed significant changes of expression for 536 genes including 20 CAZyme genes, but only four predicted chitinolytic genes that were up-regulated in stationary phase (*chi18C, chi19A, hex20B*, and *lpmo10A*). The expression of the two predicted transporters (CJA_0353 and CJA_1157) and the putative GlcNAc utilization operon genes did not change during stationary phase (**Fig. S1B** & **Table S2B**).

A previous study provided an in-depth analysis of *C. japonicus* gene expression when using purified α-chitin versus Glc (Monge *et al.*, 2018), therefore our present transcriptomic study uses crab shells (CRB) as a model complex substrate. When we compared the gene expression of CRB grown cells versus Glc grown cells during exponential growth, we found 699 genes significantly up-regulated in the CRB condition,

including 70 CAZyme-encoding genes. All nine genes predicted to encode chitin-active enzymes were up-regulated as expected in the CRB condition**.** Additionally, the two hypothetical transporters (CJA_0353 and CJA_1157) as well as the four genes of the putative GlcNAc utilization operon were highly up-regulated (**Fig. 1B, Fig. 2,** & **Table S1B**).

Gene expression analysis for CRB versus Glc cells in stationary phase identified a total of 809 up-regulated genes with 11 CAZyme-encoding genes, including five genes encoding chitin-active CAZymes (*lpmo10A*, *chi18D*, *chi18C*, *hex20B*, and *chi18A*). Interestingly, the putative transporters CJA_0353 and CJA_1157 were up-regulated while the putative GlcNAc utilization operon genes were not (**Fig. S1C** & **Table S2C**).

To further characterize the regulatory response of *C. japonicus* to complex chitin-containing biomass, we compared the gene expression profile of cells grown using CRB versus GlcNAc during exponential growth. We observed the up-regulation of 1012 genes, including 74 CAZymes in the CRB condition. Six out the nine genes predicted to encode chitin-active CAZymes were up-regulated (*lpmo10A***,** *csn46F***,** *chi18D***,** *chi19A***,** *chi18C*, and *hex20A*). The predicted transporter encoded by CJA_0353 was up-regulated, while CJA_1157 gene transcripts were highly abundant in both conditions leading to no differential expression. The putative GlcNAc utilization operon genes were down-regulated in the CRB condition (**Fig. 1C, Fig. 2,** & **Table S1C**). While comparing the stationary phase transcriptome of CRB versus GlcNAc grown cells, we identified 586 genes up-regulated and 20 CAZyme-encoding genes. Interestingly, the only gene encoding a chitin-active CAZyme up-regulated in the CRB condition was a chitosanase

gene (*csn46F*). The two transporters (CJA_0353 and CJA_1157) and the GlcNAc operon genes were not up-regulated in stationary phase for the CRB condition (**Fig. S1D** & **Table S2D**).

We next investigated *C. japonicus* gene expression during the degradation of CRB versus α-chitin during exponential growth. We observed the up-regulation of 903 genes, including 24 CAZyme-encoding genes but only two chitinase-encoding genes (*chi18C* and *csn46F*). Interestingly, three chitinase-encoding genes were down-regulated in the CRB condition (*chi18D*, *chi18B*, and *hex20A*). The remaining four genes encoding chitin-active CAZymes, the four GlcNAc operon genes, and the two putative transporters CJA_1157 and CJA_0353 were highly expressed in both conditions but none were differentially expressed in this comparison (**Fig. 1D, Fig. 2,** & **Table S1D**).

The RNAseq data for CRB versus α-chitin grown cells in stationary phase revealed up-regulation of 1115 genes, including 34 CAZyme-encoding genes. All of the genes predicted to encode chitin active CAZymes were highly expressed in both growth conditions, but the *chi18C* gene was up-regulated while the *chi18B* and *hex20A* genes were down-regulated in the CRB condition. There was no differential gene expression of CJA_0353, CJA_1157 or the four genes encoded in a putative GlcNAc utilization operon (**Fig. S1E** & **Table S2E**).

Transcriptome analysis for *C. japonicus* cells grown using α-chitin versus GlcNAc during exponential growth revealed up-regulation of 1241 gene, including 110 CAZyme genes with seven genes that encode chitin active enzymes (*csn47F, chi18D, chi19A, chi18B, chi18C, hex20A*, and *lpmo10A*). The CJA_0353 gene was up-regulated, but the

CJA_1157 gene was not in exponential phase. The GlcNAc utilization operon genes were down-regulated in exponential phase for this comparison **(Fig. 1E, Fig. 2,** & **Table S1E)**.

Transcriptome analysis for *C. japonicus* cells grown using α-chitin versus GlcNAc in stationary phase identified 654 genes up-regulated including 75 CAZyme-encoding genes. Six genes that encode chitin active enzymes were up-regulated (*lpmo10A, chi18B, chi18D, hex20A, chi19A*, and *chi18C*). The two predicted transporters (CJA_1157 and CJA_0353) and the putative GlcNAc utilization operon genes were highly expressed in both conditions, but we found that CJA_1157, *nag9A* and *nagB* were down-regulated in the α-chitin condition **(Fig. S1F** & **Table S1F)**.

Finally, when comparing the differential gene expression between exponential versus stationary phase for C. japonicus grown using CRB as the sole nutrient source we observed only five CAZyme-encoding genes were differentially expressed (*cel6A*, *pel3B*, *cbp2D*, *cbp2E*, and *lpmo10B*). There was no differential gene expression for any genes that encoded chitin active enzymes, transporters, or GlcNAc utilization (**Fig. S1G** & **Table S2G**).

While the focus of this study was on the CAZyme and transporter response of *C. japonicus* as pertains to chitin metabolism, we also surveyed the highest expressed genes, irrespective of function, in an attempt to identify any patterns (**Supplemental Materials File #2**). We observed that in the GlcNAc vs Glc and crab shells vs Glc conditions we found that proteases and stress response proteins were up-regulated. While the total number of up-regulated genes on GlcNAc vs Glc is low (42 genes), this was expected given that *N*-acetylglucosamine differs from glucose only by an

acetamide group at the C2 position. Removal of this group by a deacetlylase (*nag9A*) and a deaminase (*nagB*), both of which were up-regulated, allows for this metabolite to then enter glycolysis. Furthermore, we found that the crab shell condition had several protease and stress response genes up-regulated, which suggests that *C. japonicus* must not only extract energy from the *N*-acetylglucosamine, but also contend with the difficulties of deconstructing a complex insoluble substrate. While beyond the scope of this study, these comparisons also allow for the identification of differences between different substrate types including soluble vs insoluble (*i.e.* GlcNAc vs α-chitin) and purified vs authentic (*i.e.* α-chitin vs crab shell).

Gene loci CJA_0353 and CJA_1157 encode TonB-dependent transporters that are essential for chito-oligosaccharides import. RNAseq analysis suggested a pivotal role of two putative transporters (CJA_1157 and CJA_0353) during GlcNAc, α-chitin, and crab shell degradation. Bioinformatic analysis of these two transporters using the PFAM database (El-Gebali *et al.*, 2019) revealed the presence of two typical domains present in TonB-dependent transporters (TBDTs), which are a plug domain and an outer membrane pore domain (**Fig. 3A**). A BLAST alignment indicated that the proteins encoded by CJA_0353 and CJA_1157 shared 36% amino acid identity and 53% similarity in the predicted plug domain, but only 25% identity and 40% similarity in the predicted β-barrel domain. Interestingly, these *C. japonicus* proteins shared no amino acid similarity to the two previously characterized CusC-type TBDTs from *Flavobacterium johnsoniae* (Larsbrink *et al.*, 2016). Therefore, to establish the importance of the *C. japonicus* predicted TBDTs in chitin metabolism we generated in-

frame gene deletion strains for both CJA_0353 and CJA_1157 and performed growth analyses using α-chitin or CRB as the sole carbon source. For these experiments we included a Δ*gsp* mutant strain, which has the ten-gene operon that encode the entire general secretion pathway deleted from the genome, as a strong negative control (Gardner & Keating, 2010, Nelson & Gardner, 2015). As expected, this protein secretion deficient mutant was unable to grow using either α-chitin or CRB as a sole carbon source**.** When grown using CRB, the ΔCJA_0353 strain behaved similar to the wild-type strain in terms of its growth rate and maximum density obtained. In contrast, the ΔCJA_1157 strain displayed a lag phase that was 50 hours longer and had a 25% reduction in the maximum density obtained when compared to the wild-type despite having a similar growth rate. The most striking result using CRB as the sole nutrient source was the complete inability of a ΔCJA_0353 ΔCJA_1157 double deletion mutant to grow (**Fig. 3B** & **Table S3).** When we tested the three mutant strains using α-chitin as the sole carbon source we observed similar phenotypes as observed in CRB **(Fig. 3C** & **Table S3**). The ΔCJA_1157 strain had a lag phase that was 72 hours longer than the wild-type despite having a growth rate and a maximum density that were similar. The ΔCJA_0353 strain grew like the wild-type strain both in terms of growth rate and maximum density obtained. The double deletion ΔCJA_0353 ΔCJA_1157 mutant did not grow in the α-chitin medium.

To identify the substrates being imported into the cell by the two predicted TBDTs, we performed growth analyses using GlcNAc, chitobiose ($(GlcNAc)_2$), or chitotriose ($(GlcNAc)_3$) as the sole carbon source in combination with the TDBT deletion

mutant strains. As expected, when grown with GlcNAc (**Fig. 4A)**, the deletion strains grew similar to wild-type. Interestingly, when $(GlcNAc)_2$ was used as the sole carbon source the ΔCJA_1157 mutant strain had a growth lag that was four hours longer than the wild-type strain, but had a similar growth rate and maximum growth density. The ΔCJA_0353 mutant strain grew like wild-type on chitobiose. The ΔCJA_0353 ΔCJA_1157 double mutant strain had a growth lag that was 13 hours longer than wild-type and also had a reduced growth rate (**Fig. 4B** & **Table S4**). When using $(GlcNAc)_3$, as the sole carbon source, the ΔCJA_0353 mutant strain grew like wild-type while the single ΔCJA_1157 mutant strain had a lag phase that was three hours longer than the wild-type strain but had a similar growth rate and maximum growth density. Strikingly, the ΔCJA_0353 ΔCJA_1157 double mutant was unable to grow using chitotriose (**Fig. 4C** & **Table S4**). These growth experiments suggested that both putative TBDT genes are required for the efficient transport of chito-oligosaccharides, but the dominant transporter is CJA_1157. Consequently, we suggest naming CJA_0353 as *cttA* (chito-oligosaccharide transporter A) and CJA_1157 as *cttB* (chito-oligosaccharide transporter B).

The enzyme encoded by the *hex20B* gene is required for the efficient degradation of chito-oligosaccharides. The genome of *C. japonicus* is predicted to encode two GH20 hexosaminidases (*hex20A* and *hex20B*) (DeBoy *et al.*, 2008). We found these

putative hexosaminidases genes to be up-regulated during the degradation of GlcNAc and CRB. Furthermore, these genes were previously shown to be up-regulated when *C. japonicus* was degrading α-chitin (Monge *et al.*, 2018). Protein analysis using the PFAM and dbCAN databases, (El-Gebali *et al.*, 2019, Yin *et al.*, 2012) identified two domains in Hex20A. The first domain has a predicted α + β topology and is classified as a glycoside hydrolase 20B domain (GH20-B). The second domain in Hex20A is the catalytic $(\beta\alpha)_8$-barrel GH20 domain (GH20). Bioinformatic analysis of Hex20B found four different domains which include a putative carbohydrate binding domain (CHB-HEX-N), a glycoside hydrolase 20B domain (GH20-B), a catalytic GH20 domain (GH20), and a short C-terminal domain composed of α + β sandwich structure (CHB-Hex-C) (**Table S5**) (Tews *et al.*, 1996, Mark *et al.*, 2001a, Vaaje-Kolstad *et al.*, 2013). Using SignalP 5.0, TMHHMM 2.0, and LipoP 1.0, we determined that both Hex20A and Hex20B contain a signal peptide I (SPI) sequence, which targets this enzyme for periplasmic and possible extracellular secretion (Petersen *et al.*, 2011, Juncker *et al.*, 2003, Moller *et al.*, 2001) (**Fig. 5A**).

A previous study described the importance of the Chi18A enzyme for the latter stages of chitin metabolism (Monge *et al.*, 2018). The Chi18A chitinase has only a GH18 domain, and a recent model of chitin degradation by *C. japonicus* predicted Chi18A as an outer membrane-associated lipoprotein that degrades chito-oligosaccharides. Therefore, to place the Chi18A, Hex20A, and Hex20B enzymes in a functional context we generated mutant strains that each had the *chi18A*, *hex20A*, or *hex20B* genes deleted, respectively. We also generated every possible combination of double mutant and triple mutant, specifically Δ*chi18A* Δ*hex20A*, Δ*chi18A* Δ*hex20B*,

329 Δ*hex20A* Δ*hex20B*, and Δ*chi18A* Δ*hex20A* Δ*hex20B*. With this suite of mutants, we
330 performed growth analyses using various chitin-containing substrates. As expected,
331 when grown in GlcNAc as the only source of carbon, all strains grew like wild-type (**Fig.**
332 **5**). Surprisingly, every mutant strain grown using CRB or α-chitin also behaved like wild-
333 type (**Fig. S2**). Given that the growth experiments took between five and ten days, we
334 hypothesized that the growth rates were too slow to characterize functional redundancy
335 or that the low concentration of chito-oligosaccharides generated during CRB or α-chitin
336 degradation masked the importance of the *chi18A*, *hex20A*, and *hex20B* gene products.
337 Previous work by our group found that the chitin-specific LPMO and the Chi18BCD
338 enzymes were able to work synergistically to generate GlcNAc from insoluble chitin,
339 albeit at a slow rate (Monge *et al.*, 2018). Given the slow growth on crab shells and
340 chitin it is possible that the absence of an observable growth defect from the *hex20A*,
341 *hex20B*, or *chi18A* mutants is because the action of the LPMO and GH18 enzymes
342 extracellularly generate GlcNAc and by-pass the requirement for chito-oligosaccharide
343 degrading activity.

344 To better characterize the functional roles of the *hex20A*, *hex20B*, and *chi18A*
345 gene products we grew our suite of mutants using chito-oligosaccharides (CHOS) as
346 sole carbon sources. During $(GlcNAc)_2$ degradation (**Fig. 5C** & **Table S6**), we observed
347 that the Δ*chi18A and* Δ*hex20A* single mutant strains grew similarly to the wild-type
348 strain, as did a Δ*chi18A* Δh*ex20A* double mutant. While the Δ*hex20B* single mutant had
349 a growth rate similar to wild-type, we observed that this strain had a lag phase that was
350 three hours longer (**Table S6**). The Δ*hex20A* Δh*ex20B* double mutant displayed a
351 similar phenotype to the mutant carrying the single *hex20B* deletion. Interestingly, the

352 Δ*chi18A* Δ*hex20B* double mutant displayed a more pronounced lag phase compared to
353 wild-type. The Δ*chi18A* Δ*hex20A* Δ*hex20B* triple mutant grew similar to the Δ*chi18A*
354 Δ*hex20B* double mutant. When $(GlcNAc)_3$ was used as the sole carbon source, we
355 observed similar growth trends albeit with exacerbated lag phases for the double and
356 triple mutants (**Fig. 5D**). These results suggest that the GH20 enzymes have non-
357 redundant physiological roles, a phenomena we have observed for other *C. japonicus*
358 glycoside hydrolase families (*e.g.* GH3 and GH18) (Nelson *et al.*, 2017, Monge *et al.*,
359 2018). Overall, our gene deletion experiments indicated that the *hex20B* gene product
360 has the dominant role in the degradation of chito-oligosaccharides in *C. japonicus*.

361 While the mutational experiments in *C. japonicus* helped to prioritize the
362 importance of the GH20 CAZymes, we next wanted to determine if these enzymes were
363 equally sufficient to enable CHOS degradation. Therefore we tested the *C. japonicus*
364 GH20 enzymes as functional replacements of the *E. coli* CHOS-specific
365 phosphotransferase system (PTS) (Keyhani *et al.*, 2000). In *E. coli* CHOS are imported
366 and metabolized via a six-gene operon that contains three permeases (*chbB*, *chbC*, and
367 *chbA*) (Keyhani *et al.*, 2000), a repressor/activator (*chbR*) (Plumbridge & Pellegrini,
368 2004), a phospho-β-glucosidase (*chbF*) (Thompson *et al.*, 1999), and a chitobiose
369 deacetylase (*chbG*) (Verma & Mahadevan, 2012). The ChbG deacetylase removes a
370 single acetyl group from the reducing end of chitobiose, which is then cleaved by the
371 ChbF phospho-β-glucosidase. The ChbG enzyme is essential for growth using the
372 chito-oligosaccharides $(GlcNAc)_2$ and $(GlcNAc)_3$ in *E. coli* because this bacterium does
373 not possess any hexosaminidases (Verma & Mahadevan, 2012). Consequently, we
374 used a Δ*chbG* of *E. coli* to evaluate the ability of *chi18A*, *hex20A*, and *hex20B* gene

products to produce GlcNAc, which *E. coli* can use as a sole nutrient source (**Fig. 6A** & **Table S7**). Heterologous expression of the *hex20B* gene was able to restore the growth of *E. coli* Δ*chbG* mutant strain, both in terms of growth rate and maximum growth attained when grown using CHOS (**Fig. 6B** & **Fig. 6C**). Consistent with our *C. japonicus* mutant data, heterologous expression of *hex20A* and *chi18A* did not rescue the Δ*chbG* growth defect using CHOS, which again suggests non-redundant functions of the *C. japonicus* GH20 enzymes and a dominant role for Hex20B in the utilization of chitin degradation products.

DISCUSSION

Transcriptomic analysis suggests a substrate-sensing mechanism and coordinated regulation of CAZymes by *C. japonicus* during degradation of complex chitin-containing biomass. Over the course of this study we obtained transcriptomic profiles of *C. japonicus* when using multiple substrates with varying complexity and solubility (glucose, *N*-acetylglucosamine, purified α-chitin, and crab shells) (**Fig. 1** & **Fig. S1**). We observed increased gene expression of the nine genes predicted to encode chitin-active CAZymes during CRB utilization compared to glucose, which mirrored our previously transcriptomic studies using purified α-chitin (Monge *et al.*, 2018). Interestingly, during GlcNAc degradation we observed the up-regulation of only a sub-set of *C. japonicus* chitin specific genes (*chi18D, chi18C, hex20B*, and *chi18A*). In particular, when examining the absolute level of gene expression we found that the *hex20B* gene was often also highly expressed on chitin and crab shells, which resulted in low fold-change comparison (**Fig. 2**). Our results suggest that *Cellvibrio japonicus* has a sophisticated regulatory mechanism to up-regulate specific CAZyme genes according to substrate composition, which is consistent with our previous studies of *C. japonicus* gene regulation, specifically we have found a generalized polysaccharide degradation response for substrates, such as cellulose and chitin, where a diverse array of CAZyme genes are up-regulated (Gardner *et al.*, 2014, Monge *et al.*, 2018), and specialized responses, such as for xylan, where only a very select sub-set of CAZyme genes are up-regulated (Blake *et al.*, 2018). Similar regulatory responses have been observed in other polysaccharide-degrading microbes, including cellulosome-forming bacteria (Wilson *et al.*, 2013, Ren *et al.*, 2019), human gut symbionts (Martens

406 *et al.*, 2011), and saprophytic filamentous fungi (Miao *et al.*, 2015, Wang *et al.*, 2015)
407 where the presence of complex substrates up-regulates a specific CAZyme response.
408 The up-regulation of the *lmpo10A* gene during CRB and α-chitin, but not during GlcNAc
409 degradation, is one example of the substrate-specific regulation as lytic polysaccharide
410 monooxygenases are required only for the degradation of recalcitrant biomass (Casado
411 Lopez *et al.*, 2018, Eijsink *et al.*, 2019). As a second example, *C. japonicus* had greater
412 chitinase gene expression using purified chitin compared to crab shells (**Fig. 2**, which
413 would be expected given that the increased compositional complexity of crab shells
414 reduces the overall accessible amount of chitin and consequently production rate of
415 soluble CHOS. Related, we observed up-regulation of genes that encode CAZymes and
416 TBDTs when comparing GlcNAc vs Glc, which suggests that *N*-acetylglucosamine is a
417 metabolic trigger for *C. japonicus* to prime it chitin-degradation response. We observed
418 a decrease in the expression of the genes encoding CAZymes during stationary-phase.
419 This change in expression can be attributed to a metabolic shift due to the entrance of
420 the cells into a stationary phase (Jaishankar & Srivastava, 2017), although it is unclear
421 for *C. japonicus* if the entry into stationary phase in this experiment was due to the
422 consumption of all accessible CHOS or another metabolic restriction.

423 The family GH46 are chitosanases that are known to hydrolyze chitosan, a
424 polymer of β-1,4-linked D-glucosamine (GlcN) (Marcotte *et al.*, 1996, Saito *et al.*, 1999)
425 and most representative members of this family have been characterized from
426 *Streptomyces* and *Bacillus* sp. (Viens *et al.*, 2015). Family GH19 CAZymes, originally
427 identified in plants but also found in bacteria, are endo-chitinases that can degrade
428 chitosan but have poor activity on recalcitrant chitin (Ohno *et al.*, 1996, Heggset *et al.*,

2009, Iseli *et al.*, 1996). Although the *csn*46F and *chi19A* genes were significantly up-regulated when using chitin-containing substrates, we found that these genes did not play an essential role during α-chitin or CRB degradation in *C. japonicus* as determined by mutational analyses **(Fig. S3)**. On-going work in our laboratory will further characterize the *C. japonicus* GH46 and GH19 enzymes, and we expect those data to be part of the next refinement of our model.

Aside from chitinolytic genes, we found a diverse set of CAZyme genes highly expressed during chitin degradation (**Fig. S4**). These results are similar to those observed in other *C. japonicus* transcriptome studies, specifically for cellulose and xyloglucan degradation (Gardner *et al.*, 2014, Attia *et al.*, 2018, Larsbrink *et al.*, 2014). These data suggest a theme for *C. japonicus* polysaccharide utilization that includes regulation for simple and complex substrates. For example, in this study GlcNAc induces a specific response for CHOS metabolism, while insoluble substrates (α-chitin and crab shells) elicit a more generalized carbohydrate response. This strategy of a single polysaccharide component acting as a proxy for detection of a complex substrate has been discussed for other bacterial CAZyme systems (Gruben *et al.*, 2017, Gruninger *et al.*, 2018). In the case of crab shells, the only polysaccharide present is chitin, and as expected there was no differential chitinase gene expression between purified chitin and crab shells. Interestingly, there was differential expression of other CAZyme genes, as well as proteases and stress response genes (**Supplemental Materials File 2**). These latter two gene classes suggest that *C. japonicus* is adjusting to the pH and soluble mineral changes as crab shells are being degraded, in addition to cleaving the protein found in crab shells to better access the chitin.

The *cttA* and *cttB* genes encode transporters essential for the transport of chito-oligosaccharides. TonB-dependent transporters (TBDTs) are multi-protein complexes in Gram-negative bacteria known to actively transport and be important for the metabolism of iron, vitamins, and oligosaccharides (Blanvillain *et al.*, 2007, Noinaj *et al.*, 2010, Bolam & van den Berg, 2018, Koropatkin *et al.*, 2008, Larsbrink *et al.*, 2014). Our analysis of the *C. japonicus* genome predicted the presence of 45 outer membrane receptors that are components of TBDTs. Our RNAseq data found that two genes that encode putative TBDT outer membrane receptors (CJA_0353 and CJA_1157, now renamed as CttA and CttB, respectively) were highly expressed during chitin utilization, and therefore we characterized them further by generating single and double deletion strains. As expected, none of the deletion mutants had a growth defect using GlcNAc, and we hypothesize this is due to the presence of several Outer Member Proteins (OMP) and Major Facilitator Superfamily (MFS) transporters in *C. japonicus*, with one MFS transporter (*gluP*) located in a predicted GlcNAc utilization operon (DeBoy *et al.*, 2008). Moreover, TBDTs are known to transport large substrates from the environment, and our data provides support for CttA and CttB transporting chito-oligosaccharides. Specifically, the putative TBDT mutant strains displayed strong growth defects when grown using CHOS, α-chitin, and CRB (**Fig. 3**, **Fig. 4**, **Table S3**, & **Table S4**). These results reinforce the idea that TBDTs are highly efficient to transport the chito-oligosaccharides generated in the environment (Blanvillain *et al.*, 2007, Noinaj *et al.*, 2010). We predict that CttB has a higher affinity for CHOS than CttA and is therefore the primary mechanism for the transport of chitin degradation products. This would explain

why when the *cttA* gene is deleted we do not observed a growth defect and why when *cttB* is deleted the strain is able to still grow, albeit more slowly. The ability of the *cttA cttB* double mutant to grow using chitobiose is likely due to either this substrate being cleaved to GlcNAc extracellularly or the presence of a permissive transporter. On-going work in our lab is further characterizing the CttA and CttB transporter to characterized their specificity and affinity for CHOS. Irrespective of affinity, our results suggest the major products of *C. japonicus* chitin degradation are oligosaccharides generated extracellularly and then subsequently transported into the cell. It is likely that the *C. japonicus* is transporting CHOS with a degree of polymerization ≤6 because previously characterized TBDTs from *Xanthomonas campestris pv. Campestris* and some from *Bacteroides thetaiotaomicron* were shown to transport oligosaccharides no larger than six sugar moieties (Koropatkin *et al.*, 2008, Bolam & van den Berg, 2018, Blanvillain *et al.*, 2007, Boulanger *et al.*, 2010). However, as more recent studies have demonstrated that *B. thetaiotaomicron* has TDBTs that can transport larger malto-oligosaccharides and fructo-oligosaccharides, future work by our group will further investigate if CHOS transport by *C. japonicus* is more restricted (Foley *et al.*, 2018, Gray *et al.*, 2021, Pollet *et al.*, 2021).

Functional analysis of *C. japonicus* GH20 genes suggests non-redundant functions for CAZymes involved in chito-oligosaccharide catabolism. Hexosaminidases from the family GH20 are involved in several biological processes catalyzing the hydrolysis of *N*-acetyl-hexosaminyl residues from different substrates. As examples, hexosaminidases hydrolyze gangliosides in higher organisms (Tropak *et al.*,

2004) and act as lacto-*N*-biosidases that degrade lacto-*N*-tetraose, the main component of human milk oligosaccharides (Sakurama *et al.*, 2013, Sano *et al.*, 1992). In bacterial species, some GH20 enzymes are chitobiases that hydrolyze chitobiose (Vaaje-Kolstad *et al.*, 2013, Drouillard *et al.*, 1997). Relevant to this report, previous bioinformatic analysis of *Cellvibrio japonicus* found two GH20 enzymes, Hex20A and Hex20B, and our data here suggest a dominant role for Hex20B during the degradation of chito-oligosaccharides.

Amino acid analysis of the *C. japonicus* GH20 enzymes revealed diagnostic catalytic residues in both enzymes but suggested different domain organization and cellular location. Hex20A and Hex20B catalytic domains were compared to those of characterized chitobiases from *Serratia marcescens* (Tews *et al.*, 1996, Mayer *et al.*, 2006, Mark *et al.*, 2001b) and the β-*N*-acetylhexosaminidase from *Streptomyces coelicolor* (Thi *et al.*, 2014). Both *C. japonicus* hexosaminidases have key catalytic residues (Asp-Glu), which are preceded by a characteristic consensus motif (His-X-Gly-Gly) present in the GH20 glycoside hydrolases. Hex20A has nine out ten conserved residues known to be important for the catalytic site formation, while Hex20B has all ten of these residues (**Fig. S5)** (Tews *et al.*, 1996, Drouillard *et al.*, 1997). A structural analysis of Hex20A indicates it has two domains: GH20-B and GH20 while Hex20B had four domains: CHB_HEX_N, GH20_B, Glyco_hydro_20, and CHB_HEX_C. The structure of domain CHB_HEX_N is similar to that of the carbohydrate binding module 2 (CBM2) (Gilkes *et al.*, 1988). However, there is no evidence that the CHB_HEX_N domain supports binding to carbohydrates (Tews *et al.*, 1996). Domains GH20_B and

GH20_HEX_C do not have similarity to known domains and their physiological functions are currently unknown (Drouillard *et al.*, 1997, Tews *et al.*, 1996).

Hex20A was predicted to be a secreted enzyme, while Hex20B was predicted to contain an N-terminal transmembrane helix and be located in the periplasm (**Fig. 5A**) (Juncker *et al.*, 2003, Moller *et al.*, 2001, Petersen *et al.*, 2011). As the *C. japonicus* GH20 enzymes had different domain architecture and predicted cellular locations we wanted to determine if these CAZymes had distinct physiological roles in the cell. We also included characterization of Chi18A during CHOS catabolism because it was previously implicated with the latter stages of chitin metabolism (Monge *et al.*, 2018). Using a comprehensive mutant construction strategy, we generated every combination of single, double and triple mutant strains for the *chi18A*, *hex20A*, and *hex20B* genes and evaluated their ability to grow using both purified and complex substrates (α-chitin and crab shells). Surprisingly, all of the generated mutants grew like the wild-type on these substrates (**Fig. S2**). This result suggested both a slow generation of CHOS during insoluble chitin degradation and that one or more of these genes were dispensable for growth using chitin. To further parse the physiological functions of these genes, we tested the deletion mutant strains using chitobiose and chitotriose, which we hypothesized would reveal subtle phenotypes. Our data suggested that Hex20B is the most influential hexosaminidase in *C. japonicus* (**Fig. 5C** & **5D**). We observed that the *chi18A* gene product influenced CHOS degradation only in combination with the *hex20B* gene product. Since the ∆c*hi18A* Δ*hex20B* double mutant displayed a protracted lag phase, this result suggested synergy between the two gene products for CHOS catabolism.

543 The importance of Hex20B for CHOS degradation was further supported in
544 experiments using an *E. coli* Δ*chbG* mutant strain, and these experiments helped us
545 verify the non-redundant functions of the enzymes encoded by the *hex20A*, *hex20B* and
546 *chi18A* genes (**Fig. 6**). The heterologous expression of the *hex20B* gene allowed an *E.*
547 *coli* Δ*chbG* mutant strain to grow using CHOS, while the heterologous expression of
548 either the *hex20A* or *chi18A* genes did not rescue the *E.coli* Δ*chbG* growth defect using
549 CHOS. While it is a formal possibility that the lack of rescue in *E. coli* by the *hex20A* and
550 *chi18A* gene products is due to the enzymes not being made in an active form, we
551 argue that the *E. coli* results observed are consistent with the *C. japonicus* mutant data.
552 Therefore the physiological importance of the *hex20A* gene product remains unclear,
553 specifically in terms of CHOS metabolism. While beyond the scope of this report, kinetic
554 studies of the Hex20A and Chi18A enzymes would lend insight into the substrate
555 specificity of these CAZymes.
556
557 **An updated model of *C. japonicus* chitin utilization now includes TBDTs and a**
558 **hexosaminidase.** The hydrolysis of chitin-containing biomass has predominantly been
559 studied from a biochemical perspective (Thi *et al.*, 2014, Vaaje-Kolstad *et al.*, 2013,
560 Meekrathok & Suginta, 2016, Tews *et al.*, 1996). Consequently, our transcriptomic and
561 functional genetic studies should be broadly useful to researchers who want to
562 characterize the physiological response of complex substrate degradation by Gram-
563 negative bacteria. For example, recent work in *Flavobacterium johnsoniae* suggests
564 there is increasing interest in understanding the chitin degradation and metabolism for
565 environmentally important bacterial saprophytes (Larsbrink *et al.*, 2016). Based on our

566 results we propose a model where *Cellvibrio japonicus* is secreting chitinolytic enzymes
567 including Lpmo10A, Chi18D, Chi18C, and Chi18B as “public goods” (West *et al.*, 2007)
568 to perform the initial stages of chitin degradation, but then employing a robust TBDT
569 system (via CttA and CttB) to import the chito-oligosaccharides into the periplasmic
570 space. Hex20B and Chi18A subsequently cleave the imported chito-oligosaccharides to
571 generate GlcNAc for entry into cellular metabolism. This study expands our
572 understanding of *C. japonicus* chitin utilization and on-going work in our laboratory aims
573 to understand where the remaining predicted chitin-active enzymes (Chi19A and
574 Csn47F) play a role (**Fig. 7**).

EXPERIMENTAL PROCEDURES

Media and Growth Conditions. Overnight cultures of *Escherichia coli* strains were grown in lysogenic broth (LB) (Bertani, 1951). Overnight cultures of *Cellvibrio japonicus* strains were grown on MOPS (3-(*N*-morpholino)propanesulfonic acid)) defined media (Neidhardt *et al.*, 1974) containing 0.2% wt/vol glucose (Glc). Additional growth experiments with *C. japonicus* mutant strains used MOPS defined media with 0.25% wt/vol *N*-acetylglucosamine (GlcNAc), 0.25% wt/vol chitobiose $(GlcNAc)_2$, 0.25% chitotriose $(GlcNAc)_3$, 0.25% wt/vol α-chitin from shrimp shells (Sigma, Aldrich) or 1-10% wt/vol crab shells (*Callinectes sapidus*; CRB). The latter two substrates are completely insoluble, and to obtain substrates of a uniform size the α-chitin flakes were sieved through a 130 mm Buchner polypropylene as was done previously (Monge *et al.*, 2018). CRB pieces were sieved in a similar manner. For growth analysis studies, both *C. japonicus* and *E. coli* strains were grown for 24 hours at 30°C with a high level of aeration (225 RPM). These cultures were used at a 1:100 dilution to inoculate a 96-well assay plate, where each well contained 198 µL of MOPS defined media with a single carbon source (Glc, GlcNAc, $(GlcNAc)_2$ or $(GlcNAc)_3$). Growth in 96-well assay plates was measured as a function of the optical density at 600 nm (OD_{600}) using a Tecan M200Pro or a BioTek EPOCH2 plate reader set to 30°C with and a constant level of agitation. The CRB experiments were done in a 96-well assay plate with biomass containment devices (mBCDs) to avoid obstruction of the readings from the insoluble substrate (Monge *et al.*, 2020). To measure growth using α-chitin, 5 mL of MOPS defined media was dispensed into an 18 mm test tube containing biomass inside a biomass containment device, as done previously (Monge *et al.*, 2018). The OD_{600} was

598 measured with a Spec20D+ spectrophotometer (Thermo Scientific). All growth
599 experiments were performed in biological triplicate, and growth statistics were
600 calculated with the Prism 6 software package. Plate media used either LB or MOPS-
601 glucose and was solidified with 1.5% agar. When required, kanamycin was used at a
602 concentration of 50 µg/mL and ampicillin at a concentration of 100 µg /mL.
603
604 **Construction of *C. japonicus* and *E. coli* strains.** *C. japonicus* gene deletion mutants
605 were made and verified using previously published protocols (Nelson & Gardner, 2015,
606 Gardner & Keating, 2010). Briefly, a suicide vector was generated by cloning ±500 bp
607 up- and down-stream from the target gene into the vector pK18*mobsacB* (Schafer *et al.*,
608 1994). Tri-parental mating conjugated the suicide vector (Green & Rogers, 2013) into *C.*
609 *japonicus* using *E. coli* strains that contained either the pK18*mobsacB* vector or the
610 pRK2013 helper plasmid (Figurski & Helinski, 1979). *C. japonicus* mutant strains were
611 obtained through a selection and counter-selection scheme using kanamycin and
612 sucrose, respectively. Gene deletion mutants were then confirmed by PCR analysis.
613 For heterologous expression studies in *E. coli* JW1722 Δ*chbG*::kan, the *C.*
614 *japonicus hex20A*, *hex20B*, or *chi18A* genes were cloned into the pUC19 vector
615 (Norrander *et al.*, 1983). These vectors were then transformed into chemically
616 competent *E. coli* JW1722 strains using standard protocols (Green & Rogers, 2013).
617 **Table S8** lists all of the strains, plasmids, and primers used in this study.
618
619 **Transcriptomic analysis.** Transcriptomic analysis was conducted for *C. japonicus*
620 grown using Glc, GlcNAc, or CRB as the only source of carbon using previously

described protocols (Gardner *et al.*, 2014, Nelson *et al.*, 2017, Blake *et al.*, 2018, Monge *et al.*, 2018). Briefly, for each carbon source samples were taken in biological triplicate at two time points, with the first being early exponential (Li, 2012) phase ($0.1>OD_{600}>0.2$) and the second being stationary phase. The company GeneWiz (Plainfield, NJ) performed RNA sequencing using an Illumina HiSeq2500 (50bp single-end reads; >10 million reads per sample). The data were output as FASTQ files, which were subsequently analyzed using DESeq2 (Love *et al.*, 2014) through the GALAXY web-based platform (Blankenberg *et al.*, 2010). The following parameters were calculated: base mean, $\log_2$ (fold change), standard error of the $\log_2$(fold change), and a Benjamini-Hochberg adjusted p-value. An adjusted p-value >0.01 and a $\log_2$(fold change) >2 were selected as cut-off parameters for significance. For visualization purposes in this report a maximum threshold p-value of $1E^{-300}$ was used (*i.e.* the upper boundary of the Y-axis). All RNAseq data generated for this study have been submitted to NCBI GEO (Barrett *et al.*, 2013) under accession number GSE149593. The α-chitin RNAseq data used in this report were available from a previously study (GSE90955) (Monge *et al.*, 2018).

Bioinformatics analysis. We predicted CAZyme domains present in the GH20 enzymes using the Database for Automated Carbohydrate-active enzyme ANnotation (dbCAN) (Yin *et al.*, 2012) and PFam (Yin *et al.*, 2012). Using the LipoP 1.0 (Juncker *et al.*, 2003), SignalP 4.0 (Petersen *et al.*, 2011), and THMM (Moller *et al.*, 2001) analysis tools we derived a putative cellular location for the *C. japonicus* GH20 enzymes. The

643 enzyme domain organization images were generated using the web-based server
644 Biological Sequence Illustrator (IBS) (Liu *et al.*, 2015).
645

ACKNOWLEDGEMENTS

This work was funded by the U.S. Department of Energy, Office of Science, Office of Biological and Environmental Research under Award Number DE-SC0014183. Additional support to E.C.M. came from the Meyerhof Graduate Fellows Program (2-R25-GM55036) and the Chemistry and Biology Interface Program (T32- GM066706).

AUTHOR CONTRIBUTIONS

E.C.M. Performed the RNAseq sampling and transcriptome analysis, generated *C. japonicus* mutants and *E. coli* strains, performed the growth and physiology experiments, generated the figures, and was the lead writer of the manuscript

J.G.G. Designed the study, supervised all work performed, and contributed to writing the manuscript.

DISCLAIMER

669 expressed herein do not necessarily state or reflect those of the United States
670 Government or any agency thereof.
671
672 **COMPLIANCE WITH ETHICAL STANDARDS**
673 This article does not contain any studies using human participants or live vertebrate
674 animals. In addition, the authors declare that they have no conflict of interest.

675 **REFERENCES**
676
677 Attia, M.A., C.E. Nelson, W.A. Offen, N. Jain, G.J. Davies, J.G. Gardner & H. Brumer,
678 (2018) *In vitro* and *in vivo* characterization of three *Cellvibrio japonicus* glycoside
679 hydrolase family 5 members reveals potent xyloglucan backbone cleaving
680 functions. *Biotechnology for Biofuels* **11**: 45.
681 Barrett, T., S.E. Wilhite, P. Ledoux, C. Evangelista, I.F. Kim, M. Tomashevsky, K.A.
682 Marshall, K.H. Phillippy, P.M. Sherman, M. Holko, A. Yefanov, H. Lee, N. Zhang,
683 C.L. Robertson, N. Serova, S. Davis & A. Soboleva, (2013) NCBI GEO: archive
684 for functional genomics data sets--update. *Nucleic acids research* **41**: D991-995.
685 Beier, S. & S. Bertilsson, (2013) Bacterial chitin degradation-mechanisms and
686 ecophysiological strategies. *Frontiers in microbiology* **4**: 149.
687 Bertani, G., (1951) Studies on lysogenesis. I. The mode of phage liberation by lysogenic
688 *Escherichia coli*. *J Bacteriol* **62**: 293-300.
689 Blake, A.D., N.R. Beri, H.S. Guttman, R. Cheng & J.G. Gardner, (2018) The complex
690 physiology of *Cellvibrio japonicus* xylan degradation relies on a single
691 cytoplasmic β-xylosidase for xylo-oligosaccharide utilization. *Mol Microbiol* **107**:
692 610-622.
693 Blankenberg, D., G. Von Kuster, N. Coraor, G. Ananda, R. Lazarus, M. Mangan, A.
694 Nekrutenko & J. Taylor, (2010) Galaxy, a web-based genome analysis tool for
695 experimentalists. *Curr Protoc Mol Biol* **19**: 1-21.
696 Blanvillain, S., D. Meyer, A. Boulanger, M. Lautier, C. Guynet, N. Denance, J. Vasse, E.
697 Lauber & M. Arlat, (2007) Plant carbohydrate scavenging through tonB-

dependent receptors: a feature shared by phytopathogenic and aquatic bacteria. *PLoS One* **2**: e224.

Bolam, D.N. & B. van den Berg, (2018) TonB-dependent transport by the gut microbiota: novel aspects of an old problem. *Curr Opin Struct Biol* **51**: 35-43.

Boulanger, A., G. Dejean, M. Lautier, M. Glories, C. Zischek, M. Arlat & E. Lauber, (2010) Identification and regulation of the N-acetylglucosamine utilization pathway of the plant pathogenic bacterium *Xanthomonas campestris* pv. *campestris*. *J Bacteriol* **192**: 1487-1497.

Casado Lopez, S., M. Peng, T.Y. Issak, P. Daly, R.P. de Vries & M.R. Makela, (2018) Induction of Genes Encoding Plant Cell Wall-Degrading Carbohydrate-Active Enzymes by Lignocellulose-Derived Monosaccharides and Cellobiose in the White-Rot Fungus *Dichomitus squalens*. *Appl Environ Microbiol* **84**.

DeBoy, R.T., E.F. Mongodin, D.E. Fouts, L.E. Tailford, H. Khouri, J.B. Emerson, Y. Mohamoud, K. Watkins, B. Henrissat, H.J. Gilbert & K.E. Nelson, (2008) Insights into plant cell wall degradation from the genome sequence of the soil bacterium *Cellvibrio japonicus*. *J Bacteriol* **190**: 5455-5463.

Drouillard, S., S. Armand, G.J. Davies, C.E. Vorgias & B. Henrissat, (1997) *Serratia marcescens* chitobiase is a retaining glycosidase utilizing substrate acetamido group participation. *Biochem J* **328 (Pt 3)**: 945-949.

Eijsink, V., D. Petrovic, Z. Forsberg, S. Mekasha, Å.R. Kjendseth, A. Várnai, B. Bissaro & G. Vaaje-Kolstad, (2019) On the functional characterization of lytic polysaccharide monooxygenases (LPMOs). *Biotechnology for Biofuels* **12**.

El-Gebali, S., J. Mistry, A. Bateman, S.R. Eddy, A. Luciani, S.C. Potter, M. Qureshi, L.J. Richardson, G.A. Salazar, A. Smart, E.L.L. Sonnhammer, L. Hirsh, L. Paladin, D. Piovesan, S.C.E. Tosatto & R.D. Finn, (2019) The Pfam protein families database in 2019. *Nucleic acids research* **47**: D427-D432.

Figurski, D.H. & D.R. Helinski, (1979) Replication of an origin-containing derivative of plasmid RK2 dependent on a plasmid function provided in trans. *Proc Natl Acad Sci USA* **76**: 1648-1652.

Foley, M.H., E.C. Martens & N.M. Koropatkin, (2018) SusE facilitates starch uptake independent of starch binding in *B. thetaiotaomicron*. *Mol Microbiol* **108**: 551-566.

Forsberg, Z., C.E. Nelson, B. Dalhus, S. Mekasha, J.S. Loose, L.I. Crouch, A.K. Rohr, J.G. Gardner, V.G. Eijsink & G. Vaaje-Kolstad, (2016) Structural and functional analysis of a lytic polysaccharide monooxygenase important for efficient utilization of chitin in *Cellvibrio japonicus*. *J Biol Chem* **291**: 7300-7312.

Francesko, A. & T. Tzanov, (2011) Chitin, chitosan and derivatives for wound healing and tissue engineering. *Advances in biochemical engineering/biotechnology* **125**: 1-27.

Gooday, G.W., (1990) The ecology of chitin degradation. In: Advances in Microbial Ecology. M. K.C (ed). Boston, MA: Springer, vol. 11.

Garcia, C.A., J.A. Narrett & J.G. Gardner, (2020) Trehalose degradation in *Cellvibrio japonicus* exhibits no functional redundancy and is solely dependent on the Tre37A enzyme. *Appl. Environ. Microbiol.* **86**: e01639-01620.

741 Gardner, J.G., (2016) Polysaccharide degradation systems of the saprophytic bacterium
742 *Cellvibrio japonicus*. *World Journal of Microbiology and Biotechnology* **32**: 121-
743 132.
744 Gardner, J.G., L. Crouch, A. Labourel, Z. Forsberg, Y.V. Bukhman, G. Vaaje□Kolstad,
745 H.J. Gilbert & D.H. Keating, (2014) Systems biology defines the biological
746 significance of redox□active proteins during cellulose degradation in an aerobic
747 bacterium. *Mol Microbiol* **94**: 1121-1133.
748 Gardner, J.G. & D.H. Keating, (2010) Requirement of the type II secretion system for
749 utilization of cellulosic substrates by *Cellvibrio japonicus*. *Appl. Environ.*
750 *Microbiol.* **76**: 5079-5087.
751 Gilkes, N.R., R.A. Warren, R.C. Miller, Jr. & D.G. Kilburn, (1988) Precise excision of the
752 cellulose binding domains from two *Cellulomonas fimi* cellulases by a
753 homologous protease and the effect on catalysis. *J Biol Chem* **263**: 10401-
754 10407.
755 Gopal, J., M. Muthu, T. Dhakshanamurthy, K.J. Kim, N. Hasan, S.J. Kwon & S. Chun,
756 (2019) Sustainable ecofriendly phytoextract mediated one pot green recovery of
757 chitosan. *Scientific Reports* **9**: 13832.
758 Gortari, M.C. & R.A. Hours, (2013) Biotechnological processes for chitin recovery out of
759 crustacean waste: A mini-review. *Electron J Biotechn* **16**.
760 Gray, D.A., J.R. White, A.O. Oluwole, P. Rath, A.J. Glenwright, A. Mazur, M. Zahn, A.
761 Basle, C. Morland, S.L. Evans, A. Cartmell, C.V. Robinson, S. Hiller, N.A.
762 Ranson, D.N. Bolam & B. van den Berg, (2021) Insights into SusCD-mediated
763 glycan import by a prominent gut symbiont. *Nature Communications* **12**: 44.

764 Green, R. & E.J. Rogers, (2013) Transformation of chemically competent *E. coli*.
765 *Methods Enzymol* **529**: 329-336.
766 Gruben, B.S., M.R. Mäkelä, J.E. Kowalczyk, M. Zhou, I. Benoit-Gelber & R.P. De Vries,
767 (2017) Expression-based clustering of CAZyme-encoding genes of *Aspergillus*
768 *niger*. *BMC Genomics* **18**: 900.
769 Gruninger, R.J., T.T.M. Nguyen, I.D. Reid, J.L. Yanke, P. Wang, D.W. Abbott, A. Tsang
770 & T. McAllister, (2018) Application of transcriptomics to compare the
771 Carbohydrate Active enZymes that are expressed by diverse genera of
772 anaerobic fungi to degrade plant cell wall carbohydrates. *Frontiers in*
773 *microbiology* **9**: 1581.
774 Heggset, E.B., I.A. Hoell, M. Kristoffersen, V.G.H. Eijsink & K.M. Vårum, (2009)
775 Degradation of chitosans with chitinase G from *Streptomyces coelicolor* A3(2):
776 Production of chito-oligosaccharides and insight into subsite specificities.
777 *Biomacromolecules* **10**: 892-899.
778 Ifuku, S., (2014) Chitin and Chitosan Nanofibers: Preparation and Chemical
779 Modifications *Molecules* **19**: 18367-18380.
780 Iseli, B., S. Armand, T. Boller, J.-M. Neuhaus & B. Henrissat, (1996) Plant chitinases
781 use two different hydrolytic mechanisms. *FEBS Letters* **382**: 186-188.
782 Jaishankar, J. & P. Srivastava, (2017) Molecular Basis of Stationary Phase Survival and
783 Applications. *Frontiers in microbiology* **8**: 2000.
784 Juncker, A.S., H. Willenbrock, G. Von Heijne, S. Brunak, H. Nielsen & A. Krogh, (2003)
785 Prediction of lipoprotein signal peptides in Gram-negative bacteria. *Protein*
786 *science : a publication of the Protein Society* **12**: 1652-1662.

787 Keyhani, N.O., L.X. Wang, Y.C. Lee & S. Roseman, (2000) The chitin disaccharide,
788 N,N'-diacetylchitobiose, is catabolized by *Escherichia coli* and is
789 transported/phosphorylated by the phosphoenolpyruvate:glycose
790 phosphotransferase system. *J Biol Chem* **275**: 33084-33090.
791 Khor, E. & L.Y. Lim, (2003) Implantable applications of chitin and chitosan. *Biomaterials*
792 **24**: 2339-2349.
793 Koropatkin, N.M., E.C. Martens, J.I. Gordon & T.J. Smith, (2008) Starch catabolism by a
794 prominent human gut symbiont is directed by the recognition of amylose helices.
795 *Structure* **16**: 1105-1115.
796 Lacombe-Harvey, M., R. Brzezinski & C. Beaulieu, (2018) Chitinolytic functions in
797 actinobacteria: ecology, enzymes, and evolution. *Appl Microbiol Biotechnol* **102**:
798 7219-7230.
799 Larsbrink, J., A.J. Thompson, M. Lundqvist, J.G. Gardner, G.J. Davies & H. Brumer,
800 (2014) A complex gene locus enables xyloglucan utilization in the model
801 saprophyte *Cellvibrio japonicus*. *Mol Microbiol* **94**: 418-433.
802 Larsbrink, J., Y. Zhu, S.S. Kharade, K.J. Kwiatkowski, V.G. Eijsink, N.M. Koropatkin,
803 M.J. McBride & P.B. Pope, (2016) A polysaccharide utilization locus from
804 *Flavobacterium johnsoniae* enables conversion of recalcitrant chitin.
805 *Biotechnology for Biofuels* **9**: 260.
806 Li, W., (2012) Volcano plots in analyzing differential expressions with mRNA
807 microarrays. *J Bioinform Comput Biol* **10**: 1231003.

808 Liu, W., Y. Xie, J. Ma, X. Luo, P. Nie, Z. Zuo, U. Lahrmann, Q. Zhao, Y. Zheng, Y. Zhao,
809 Y. Xue & J. Ren, (2015) IBS: an illustrator for the presentation and visualization
810 of biological sequences. *Bioinformatics* **31**: 3359-3361.
811 Lombard, V., H. Golaconda Ramulu, E. Drula, P.M. Coutinho & B. Henrissat, (2014)
812 The Carbohydrate-Active enZymes database (CAZy) in 2013. *Nucleic acids*
813 *research* **42**: D490-495.
814 Love, M.I., W. Huber & S. Anders, (2014) Moderated estimation of fold change and
815 dispersion for RNA-seq data with DESeq2. *Genome Biology* **15**: 550.
816 Marcotte, E.M., A.F. Monzingo, S.R. Ernst, R. Brzezinski & J.D. Robertus, (1996) X-ray
817 structure of an anti-fungal chitosanase from streptomyces N174. *Nat Struct Biol*
818 **3**: 155-162.
819 Mark, B.L., D.J. Vocadlo, S. Knapp, B.L. Triggs-Raine, S.G. Withers & M.N. James,
820 (2001a) Crystallographic evidence for substrate-assisted catalysis in a bacterial
821 beta-hexosaminidase. *J Biol Chem* **276**: 10330-10337.
822 Mark, B.L., D.J. Vocadlo, S. Knapp, B.L. Triggs-Raine, S.G. Withers & M.N.G. James,
823 (2001b) Crystallographic evidence for substrate-assisted catalysis in a bacterial
824 β-hexosaminidase. *J Biol Chem*.
825 Martens, E.C., E.C. Lowe, H. Chiang, N.A. Pudlo, M. Wu, N.P. McNulty, D.W. Abbott, B.
826 Henrissat, H.J. Gilbert, D.N. Bolam & J.I. Gordon, (2011) Recognition and
827 degradation of plant cell wall polysaccharides by two human gut symbionts.
828 *PLOS Biology* **12**: e1001221.

829 Matroodi, S., M. Motallebi, M. Zamani & M. Moradyar, (2013) Designing a new chitinase
830 with more chitin binding and antifungal activity. *World J Microbiol Biotechnol* **29**:
831 1517-1523.
832 Mayer, C., D.J. Vocadlo, M. Mah, K. Rupitz, D. Stoll, R.A. Warren & S.G. Withers,
833 (2006) Characterization of a β--N-acetylhexosaminidase and a β-N-
834 acetylglucosaminidase/β--glucosidase from *Cellulomonas fimi*. *FEBS J* **273**:
835 2929-2941.
836 Meekrathok, P. & W. Suginta, (2016) Probing the Catalytic Mechanism of Vibrio harveyi
837 GH20 β-N-Acetylglucosaminidase by Chemical Rescue. In: PLoS One. pp.
838 Meibom, K.L., X.B. Li, A.T. Nielsen, C.Y. Wu, S. Roseman & G.K. Schoolnik, (2004)
839 The *Vibrio cholerae* chitin utilization program. *Proc Natl Acad Sci U S A* **101**:
840 2524-2529.
841 Miao, Y., D. Liu, G. Li, P. Li, Y. Xu, Q. Shen & R. Zhang, (2015) Genome-wide
842 transcriptomic analysis of a superior biomass-degrading strain of *A. fumigatus*
843 revealed active lignocellulose-degrading genes. *BMC Genomics* **16**: 459.
844 Moller, S., M.D. Croning & R. Apweiler, (2001) Evaluation of methods for the prediction
845 of membrane spanning regions. *Bioinformatics* **17**: 646-653.
846 Monge, E.C., M. Levi, J.N. Forbin, M.D. Legesse, B.A. Udo, T.N. deCarvalho & J.G.
847 Gardner, (2020) High-throughput screening of environmental polysaccharide-
848 degrading bacteria using biomass containment and complex insoluble
849 substrates. *Applied Microbiology and Biotechnology* **104**: 3379-3389.
850 Monge, E.C., T.R. Tuveng, G. Vaaje-Kolstad, V.G.H. Eijsink & J.G. Gardner, (2018)
851 Systems analysis of the glycoside hydrolase family 18 enzymes from *Cellvibrio*

japonicus characterizes essential chitin degradation functions. *J Biol Chem* **293**: 3849-3859.

Moussian, B., (2019) Chitin: Structure, Chemistry and Biology. *Adv Exp Med Biol* **1142**: 5-18.

Neidhardt, F.C., P.L. Bloch & D.F. Smith, (1974) Culture medium for enterobacteria. *J Bacteriol* **119**: 736-747.

Nelson, C.E. & J.G. Gardner, (2015) In-frame deletions allow functional characterization of complex cellulose degradation phenotypes in *Cellvibrio japonicus*. *Appl. Environ. Microbiol.* **81** 5968-5975.

Nelson, C.E., A. Rogowski, C. Morland, J.A. Wilhide, H.J. Gilbert & J.G. Gardner, (2017) Systems analysis in *Cellvibrio japonicus* resolves predicted redundancy of β-glucosidases and determines essential physiological functions. *Mol Microbiol* **104**: 294-305.

Nguyen, S.T.C., H.L. Freund, J. Kasanjian & R. Berlemont, (2018) Function, distribution, and annotation of characterized cellulases, xylanases, and chitinases from CAZy. *Appl Microbiol Biotechnol* **102**: 1629-1637.

Noinaj, N., M. Guillier, T.J. Barnard & S.K. Buchanan, (2010) TonB-dependent transporters: regulation, structure, and function. *Annu Rev Microbiol* **64**: 43-60.

Norrander, J., T. Kempe & J. Messing, (1983) Construction of improved M13 vectors using oligodeoxynucleotide-directed mutagenesis. *Gene* **26**: 101-106.

Ohno, T., S. Armand, T. Hata, N. Nikaidou, B. Henrissat, M. Mitsutomi & T. Watanabe, (1996) A modular family 19 chitinase found in the prokaryotic organism Streptomyces griseus HUT 6037. *J Bacteriol* **178**: 5065-5070.

875 Petersen, T.N., S. Brunak, G.v. Heijne & H. Nielsen, (2011) SignalP 4.0: discriminating
876 signal peptides from transmembrane regions. *Nature Methods* **8**: 785-786.
877 Plumbridge, J. & O. Pellegrini, (2004) Expression of the chitobiose operon of
878 *Escherichia coli* is regulated by three transcription factors: NagC, ChbR and
879 CAP. *Mol Microbiol* **52**: 437-449.
880 Pollet, R.M., L.M. Martin & N.M. Koropatkin, (2021) TonB-dependent transporters in the
881 Bacteroidetes: Unique domain structures and potential functions. *Mol Microbiol*.
882 Raabe, D., C. Sachs & P. Romano, (2005) The crustacean exoskeleton as an example
883 of a structurally and mechanically graded biological nanocomposite material.
884 *Acta Materialia* **53**: 4281-4292.
885 Ren, Z., W. You, S. Wu, A. Poetsch & C. Xu, (2019) Secretomic analyses of
886 *Ruminiclostridium papyrosolvens* reveal its enzymatic basis for lignocellulose
887 degradation. *Biotechnology for Biofuels* **12**: 183.
888 Saito, J., A. Kita, Y. Higuchi, Y. Nagata, A. Ando & K. Miki, (1999) Crystal structure of
889 chitosanase from *Bacillus circulans* MH-K1 at 1.6-A resolution and its substrate
890 recognition mechanism. *J Biol Chem* **274**: 30818-30825.
891 Sakurama, H., M. Kiyohara, J. Wada, Y. Honda, M. Yamaguchi, S. Fukiya, A. Yokota,
892 H. Ashida, H. Kumagai, M. Kitaoka, K. Yamamoto & T. Katayama, (2013) Lacto-
893 N-biosidase encoded by a novel gene of *Bifidobacterium longum* subspecies
894 longum shows unique substrate specificity and requires a designated chaperone
895 for its active expression. *J Biol Chem* **288**: 25194-25206.
896 Sano, M., K. Hayakawa & I. Kato, (1992) An enzyme releasing lacto-N-biose from
897 oligosaccharides. *Proc Natl Acad Sci U.S.A* **89**: 8512-8516.

898 Satari, B. & K. Karimi, (2018) Mucoralean fungi for sustainable production of bioethanol
899 and biologically active molecules. *Appl Microbiol Biotechnol* **102**: 1097-1117.
900 Schafer, A., A. Tauch, W. Jager, J. Kalinowski, G. Thierbach & A. Puhler, (1994) Small
901 mobilizable multi-purpose cloning vectors derived from the *Escherichia coli*
902 plasmids pK18 and pK19: selection of defined deletions in the chromosome of
903 *Corynebacterium glutamicum*. *Gene* **145**: 69-73.
904 Stoykov, Y.M., A.I. Pavlov & A.I. Krastanov, (2015) Chitinase biotechnology: Production,
905 purification, and application. *Eng Life Sci* **15**: 30-38.
906 Tews, I., A. Perrakis, A. Oppenheim, Z. Dauter, K.S. Wilson & C.E. Vorgias, (1996)
907 Bacterial chitobiase structure provides insight into catalytic mechanism and the
908 basis of Tay-Sachs disease. *Nat Struct Biol* **3**: 638-648.
909 Tharanathan, R.N. & F.S. Kittur, (2003) Chitin--the undisputed biomolecule of great
910 potential. *Critical reviews in food science and nutrition* **43**: 61-87.
911 Thi, N.N., W.A. Offen, F. Shareck, G.J. Davies & N. Doucet, (2014) Structure and
912 activity of the *Streptomyces coelicolor* A3(2) β-N-acetylhexosaminidase provides
913 further insight into GH20 family catalysis and inhibition. *Biochemistry* **53**: 1789-
914 1800.
915 Thompson, J., S.B. Ruvinov, D.I. Freedberg & B.G. Hall, (1999) Cellobiose-6-phosphate
916 hydrolase (CelF) of *Escherichia coli*: characterization and assignment to the
917 unusual family 4 of glycosylhydrolases. *J Bacteriol* **181**: 7339-7345.
918 Tropak, M.B., S.P. Reid, M. Guiral, S.G. Withers & D. Mahuran, (2004) Pharmacological
919 enhancement of beta-hexosaminidase activity in fibroblasts from adult Tay-Sachs
920 and Sandhoff Patients. *J Biol Chem* **279**: 13478-13487.

Tuveng, T.R., M.O. Arntzen, O. Bengtsson, J.G. Gardner, G. Vaaje-Kolstad & V.G. Eijsink, (2016) Proteomic investigation of the secretome of *Cellvibrio japonicus* during growth on chitin. *Proteomics* **16**: 1904-1914.

Vaaje-Kolstad, G., S.J. Horn, M. Sorlie & V.G. Eijsink, (2013) The chitinolytic machinery of *Serratia marcescens*--a model system for enzymatic degradation of recalcitrant polysaccharides. *FEBS J.* **280**: 3028-3049.

Vaaje-Kolstad, G., D.R. Houston, A.H.K. Riemen, V.G.H. Eijsink & D.M.F.v. Aalten, (2005) Crystal structure and binding properties of the *Serratia marcescens* chitin-binding protein CBP21. *J Biol Chem* **280**: 11313-11319.

Verma, S.C. & S. Mahadevan, (2012) The *chbG* gene of the chitobiose (chb) operon of *Escherichia coli* encodes a chitooligosaccharide deacetylase. *J Bacteriol* **194**: 4959-4971.

Viens, P., M.E. Lacombe-Harvey & R. Brzezinski, (2015) Chitosanases from Family 46 of Glycoside Hydrolases: From Proteins to Phenotypes. *Mar Drugs* **13**: 6566-6587.

Wang, B., P. Cai, W. Sun, J. Li, C. Tian & Y. Ma, (2015) A transcriptomic analysis of *Neurospora crassa* using five major crop residues and the novel role of the sporulation regulator rca-1 in lignocellulase production. *Biotechnology for Biofuels* **8**: 21.

West, S.A., S.P. Diggle, A. Buckling, A. Gardner & A.S. Griffin, (2007) The social lives of microbes. *Annual review of ecology, evolution, and systematics* **38**: 53-77.

Wilson, C.M., M. Rodriguez, C.M. Johnson, S.L. Martin, T.M. Chu, R.D. Wolfinger, L.J. Hauser, M.L. Land, D.M. Klingeman, M.H. Syed, A.J. Ragauskas, T.J.

944 Tschaplinski, J.R. Mielenz & S.D. Brown, (2013) Global transcriptome analysis of
945 *Clostridium thermocellum* ATCC 27405 during growth on dilute acid pretreated
946 Populus and switchgrass. *Biotechnology for Biofuels* **6**: 179.
947 Yan, N. & X. Chen, (2015) Sustainability: Don't waste seafood waste. *Nature* **524**: 155-
948 157.
949 Yin, Y., X. Mao, J. Yang, X. Chen, F. Mao & Y. Xu, (2012) dbCAN: a web resource for
950 automated carbohydrate-active enzyme annotation. *Nucleic acids research* **40**:
951 w445-451.
952 Zhu, Z., T. Zheng, R.J. Homer, Y.K. Kim, N.Y. Chen, L. Cohn, Q. Hamid & J.A. Elias,
953 (2004) Acidic mammalian chitinase in asthmatic Th2 inflammation and IL-13
954 pathway activation. *Science* **304**: 1678-1682.
955
956
957

FIGURES

Figure 1. Differential gene expression for *C. japonicus* during growth in different substrates. The volcano plots show the [$\log_2$(fold change expression)] plotted against the -[$\log_{10}$(p-value)] for every gene in *C. japonicus* during exponential phase growth when using *N*-acetylglucosamine (GlcNAc) compared to glucose (Glc) **(A).** We also compared the change on gene expression for crab shell (CRB) compared to glucose (Glc) **(B)**, *N*-acetylglucosamine (GlcNAc) compared to glucose (Glc) **(C),** and α-chitin compared to glucose (Glc) **(D)**. Transcriptomic analysis of α-chitin versus GlcNAc during exponential phase **(E)** is also presented. Each gray circle represents the expression of a single *C. japonicus* gene. The black dashed lines indicate the significance cut-off values: $\log_2$(fold change) >2 and adjusted p-value of $\log_{10}$(p-value) >2. A p-value <0.01 was selected as the significance cut-off value. The genes colored red represent up-regulated genes that encode CAZymes, and the complete list of these genes can be found in **Table S1.** Genes encoding chitin active enzymes are colored orange, genes predicted to encode proteins in a putative GlcNAc utilization operon are colored green, and two TonB-dependent receptors (CJA_0353 and CJA_1157) are colored blue. For visualization purposes in this figure a maximum threshold p-value of $1E^{-300}$ was used (*i.e.* the upper boundary of the Y-axis).

Figure 2. Heat map of *C. japonicus* chitinolytic CAZyme-encoding genes expressed using different transcriptomic comparisons during exponential (A) or stationary (B) phase growth. For each growth phase the following changes of expression are presented: crab shell (CRB) versus glucose (Glc) **(A1,B1)**, *N*-

acetylglucosamine (GlcNAc) **(A2,B2)** and α-chitin **(A3,B3).** We also compared differential expression of α-chitin versus Glc **(A4,B4)** and GlcNAc **(A5,B5).** The transcriptome of GlcNAc versus glucose (**A6,B6**) is also presented. The intensity of the red color in the heat map indicates $\log_2$ (fold change) (LFC) ranging from deep red (LFC=7) to green (LFC=-2.6). Locus IDs from DeBoy *et al.,* 2009 were used to identify the genes. The α-chitin RNAseq data was obtained from Monge *et al.,* 2018.

Figure 3. Two genes encoding putative transporters *cttA* (CJA_0353) and *cttB* (CJA_1157) are required for efficient growth of *C. japonicus* in crab shell and α-chitin. Domain architecture of the two predicted TonB-dependent receptors CttA (CJA_0353) and CttB (CJA_1157). Growth analysis of deletion mutants on MOPS minimal medium supplemented with 10% (w:v) CRB **(B)** or 0.25% (w:v) α-chitin **(C).** All experiments were performed in biological triplicates; error bars represent standard deviation. Growth rates and maximum growth attained can be found in Supplemental Table S3.

Figure 4. The *cttA* (CJA_0353) and *cttB* (CJA_1157) gene products are required for efficient transport of chito-oligomers in *C. japonicus*. Deletion mutants were grown using MOPS minimal medium supplemented with 0.25% (w:v) *N*-acetylglucosamine (GlcNAc) **(A)**, 0.25% (w:v) chitobiose ($(GlcNAc)_2$) **(B)**, or 0.25% (w:v) chitotriose ($(GlcNAc)_3$) **(C)**. All growth experiments were performed in biological triplicates; error bars represent standard deviations, but in many cases are too small to

be observed. Growth rates and maximum growth attained can be found in Supplemental Table S4.

Figure 5. The *hex20B* gene product is important for the metabolism of chito-oligosaccharides. Domains of the family GH20 hexosaminidases of *C. japonicus* **(A)**. The indicated domains are as follows: a putative carbohydrate binding domain (CHB_HEX_N), a glycoside hydrolase 20B domain (GH20_B), a catalytic GH20 domain (Glyco_hydro_20), and a C-terminal domain composed of α + β sandwich structure (CHB_Hex_C). Growth analysis of deletion mutants was perfomed in MOPS minimal medium supplemented 0.25% (w:v) *N*-acetylglucosamine (GlcNAc) **(B)**, 0.25% (w:v) chitobiose $((GlcNAc)_2)$ **(C)**, or 0.25% (w:v) chitotriose $((GlcNAc)_3)$ **(D)**. The growth experiments were performed in biological triplicates; error bars represent standard deviations, but in many cases are too small to be observed. Growth rates and maximum growth attained can be found in Supplemental Table S6.

Figure 6. Heterologous expression of *Cellvibrio japonicus hex20B* in an *E. coli* Δ*chbG* mutant rescues growth defects using chito-oligosaccharides. *E. coli* strains derived from BW25113 were grown using MOPS minimal medium supplemented with 0.25% (w:v) *N*-acetylglucosamine (GlcNAc) **(A)**, 0.25% (w:v) chitobiose $((GlcNAc)_2)$ **(B)**, or 0.25% (w:v) chitotriose $((GlcNAc)_3)$ **(C)**. An empty pUC19 vector (pVOC) was included as the negative control. These growth experiments were performed in biological triplicates; error bars represent standard deviations, but in many cases are

too small to be observed. Growth rates and maximum growth attained can be found in Supplemental Table S7.

Figure 7. Updated model for chitin utilization in *C. japonicus*. Lpmo10A (green triangle) and Chi18D (orange) work together to disrupt the crystalline structure of chitin and degrade recalcitrant chitin polymers (Forsberg *et al.*, 2016, Monge *et al.*, 2018). The Chi18B and Chi18C CAZymes degrade solvent exposed chitin polymers to generate chito-oligosaccharides (CHOS), which are transported into the periplasm space by CttA and CttB. As the TonB and ExbBD inner membrane components of the CttA and CttB transport system have yet to be identified they are not shown in the model. The Chi18A CAZyme degrades the CHOS to GlcNAc in the periplasmic space. The exact location of the Hex20A and Hex20B enzymes are not well defined, but due to the presence of an SPI signal sequence are either in the periplasm or extracellular. The physiological roles for the Hex20A, Chi19A, and Csn47F CAZymes (locations of the latter two enzymes were predicted based on SignalP analysis) are unknown and currently under investigation.

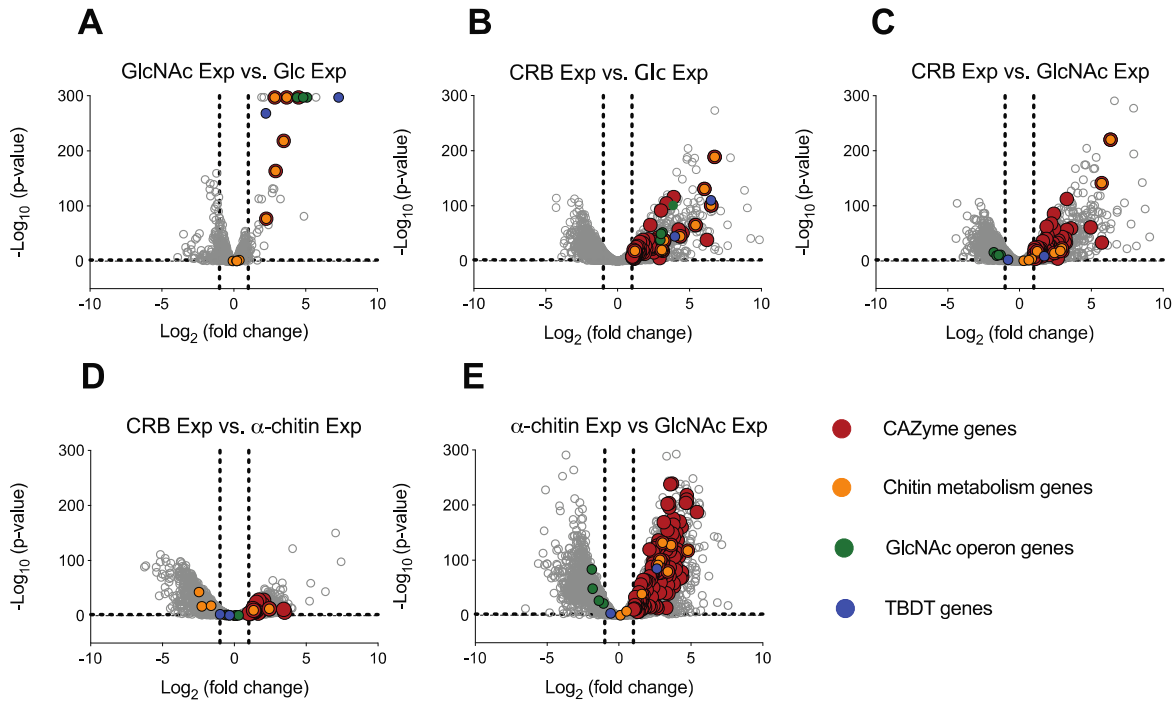
A
GlcNAc Exp vs. Glc Exp
B
CRB Exp vs. Glc Exp
C
CRB Exp vs. GlcNAc Exp
D
CRB Exp vs. α-chitin Exp
E
α-chitin Exp vs GlcNAc Exp
-Log10 (p-value)
Log2 (fold change)
CAZyme genes
Chitin metabolism genes
GlcNAc operon genes
TBDT genes

1041

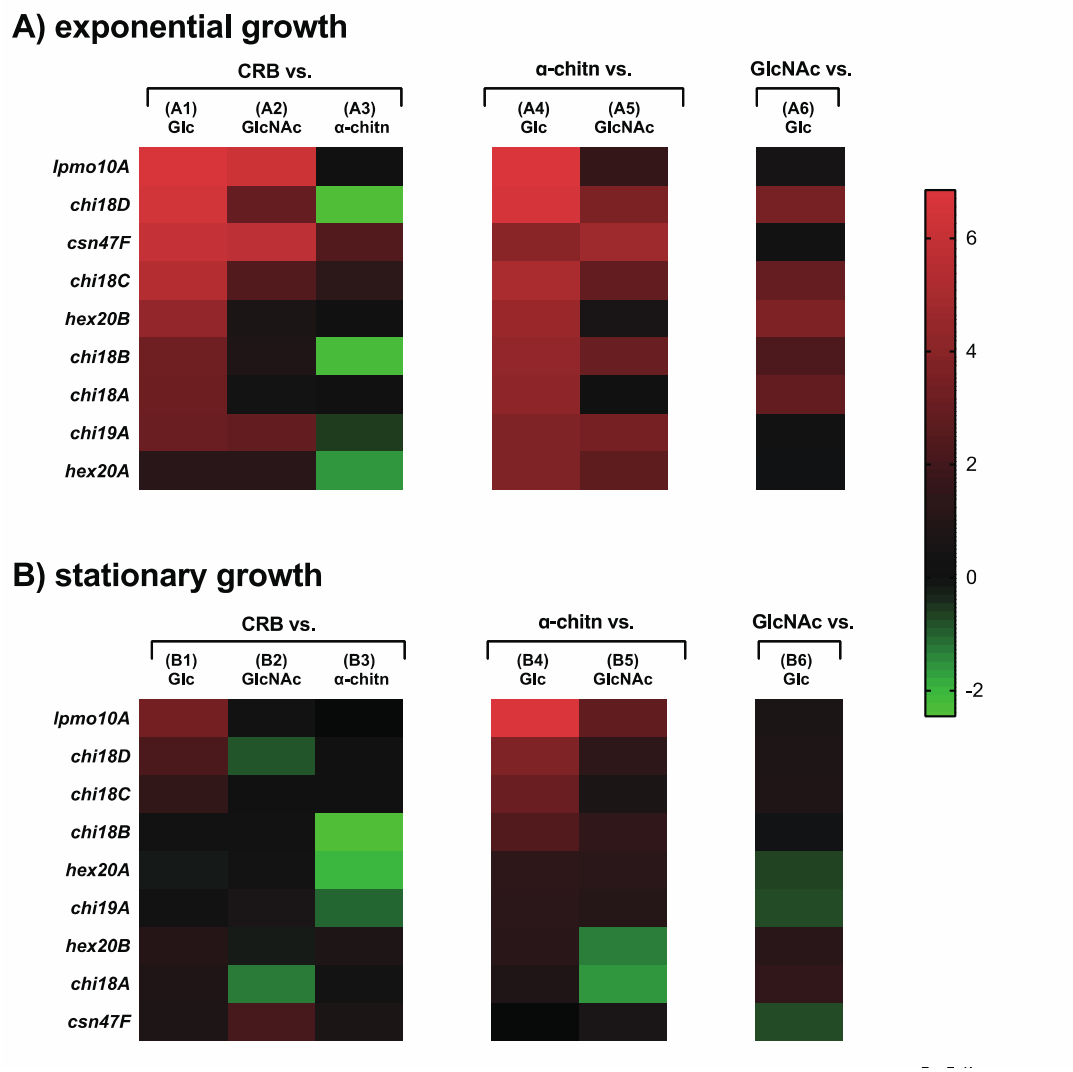

1042
1043
1044

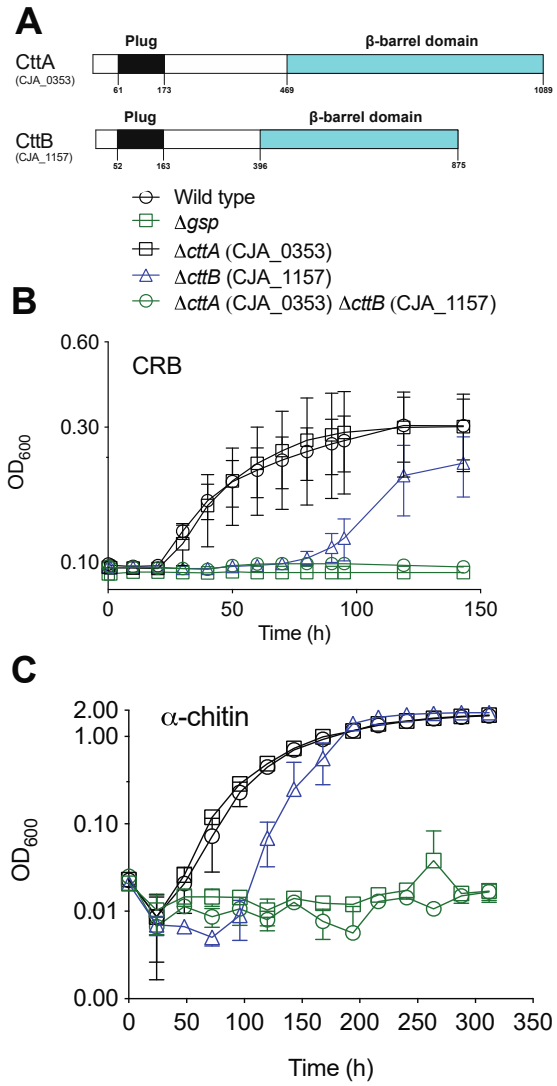

1045
1046
1047

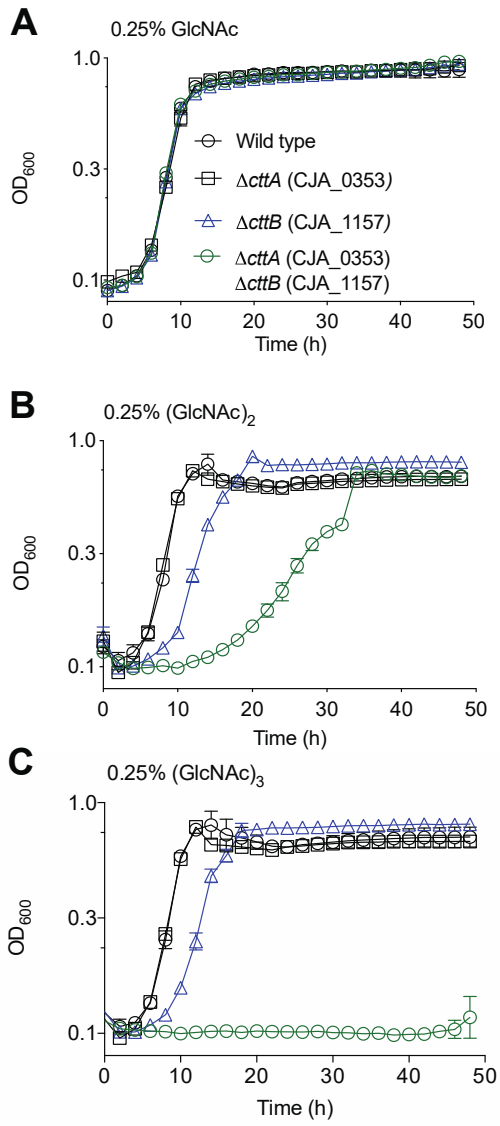

1048
1049
1050

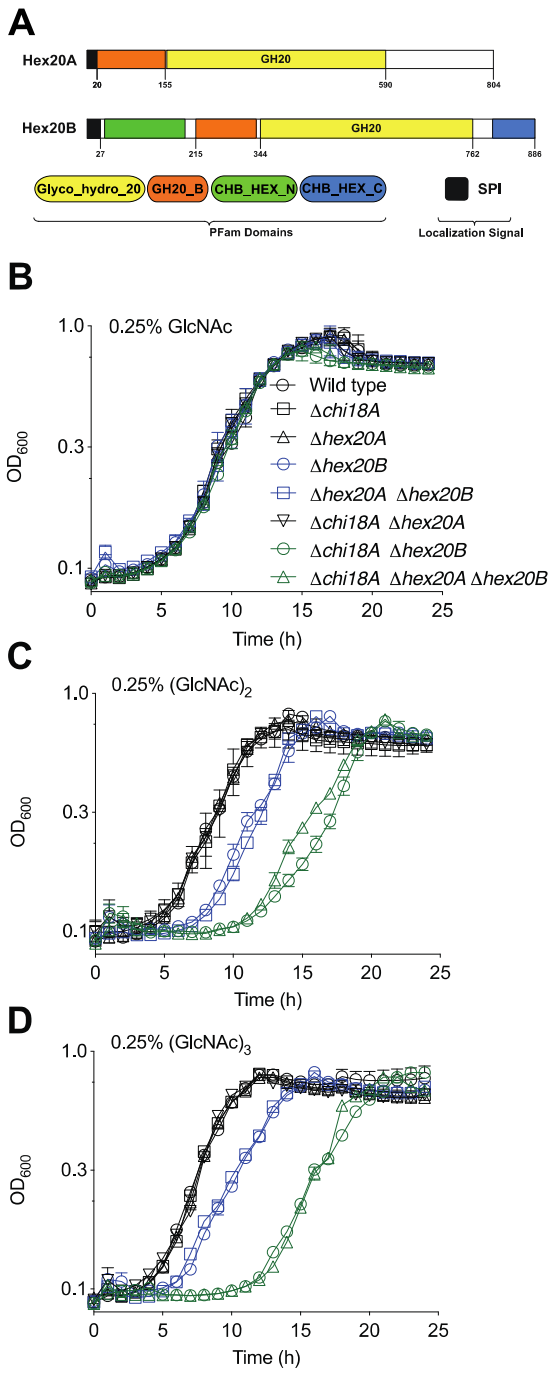

1051
1052
1053

1054

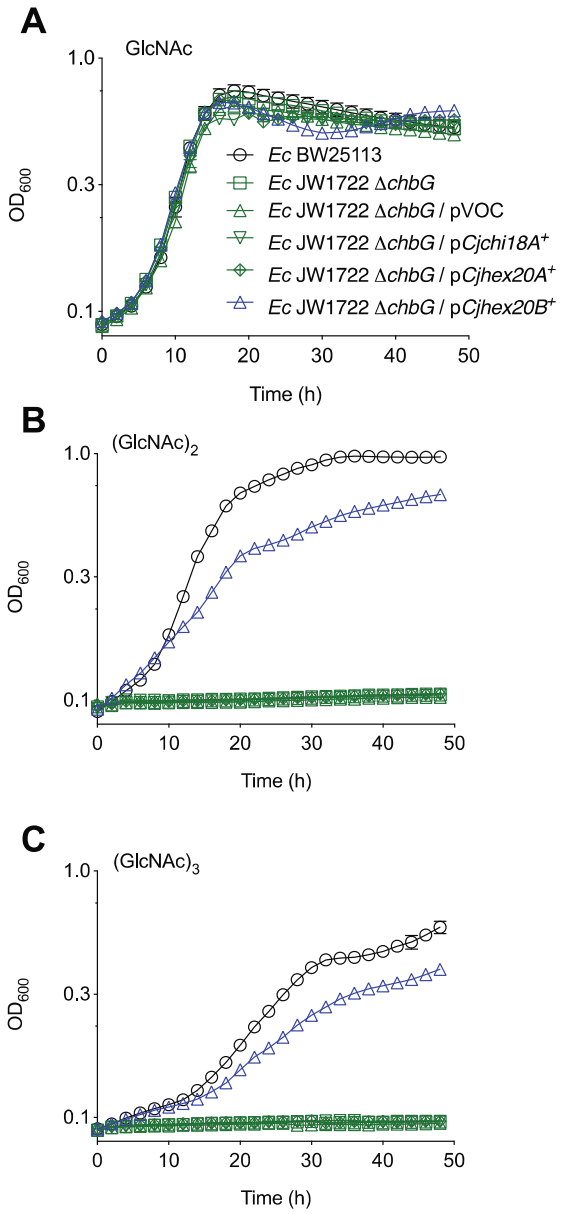

1055
1056
1057

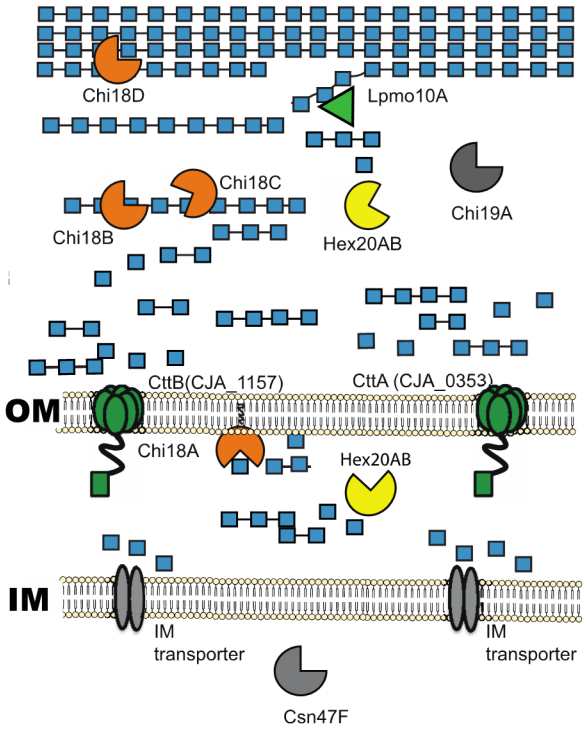
Chi18D
Lpmo10A
Chi18C
Chi18B
Hex20AB
Chi19A
CttB(CJA_1157)
CttA (CJA_0353)
OM
Chi18A
Hex20AB
IM
IM
transporter
IM
transporter
Csn47F

1058